Isomeric yield ratios in the photoproduction of ^{52m,g}Mn from natural iron

Nguyen Van Do[a], Pham Duc Khue[a], Kim Tien Thanh[a] , Md. Shakilur Rahman[b], Kyung-Sook Kim[b], Guinyun Kim[b,†], Hee-Seock Lee[c], Moo-Hyun Cho[c], In Soo Ko[c], and Won Namkung[c]

[a] *Institute of Physics, Vietnam Academy of Science and Technology,10 Dao Tan, Hanoi, Viet Nam*

[b] *Department of Physics, Kyungpook National University,1370 Sankyuk-dong, Buk-gu, Daegu 702-701, Korea*

[c] *Pohang Accelerator Laboratory, Pohang University of Science and Technology, Pohang 790 – 784, Korea*

Abstract: The isomeric yield ratios for the ^{nat}Fe(γ,xn1p)^{52m,g}Mn reactions have been measured by the activation and the γ-ray spectroscopic methods at 50-, 60-, 70-MeV, and 2.5-GeV bremsstrahlung energies. The high purity natural iron foils in disc shape were irradiated with uncollimated bremsstrahlung beams of the Pohang Accelerator Laboratory. The induced activities in the irradiated foils were measured by the high-resolution γ-ray spectrometry with a calibrated high-purity Germanium (HPGe) detector. In order to improve the accuracy of the experimental results the necessary corrections were made in the gamma activity measurements and data analysis. The obtained isomeric yield ratios for the ^{nat}Fe(γ,xn1p)^{52m,g}Mn reactions at 50-, 60-, 70-MeV, and 2.5-GeV bremsstrahlung energies are 0.27 ± 0.03, 0.33 ± 0.04, 0.34 ± 0.04, and 1.25 ± 0.15, respectively. The present results at 50-, 60-MeV, and 2.5-GeV bremsstrahlung energies are the first measurements. We found that the isomeric yield ratio of the ^{nat}Fe(γ,xn1p)^{52m,g}Mn reaction depends on the incident bremsstrahlung energy and the mass difference between the product and the target nucleus when we compared the present results with other experimental data at different energies.

1. Introduction

Isomeric yield ratios are of fundamental interest because they are useful for various studies related to nuclear reaction and nuclear structure such as transfer of angular momentum, spin dependence of nuclear level density, refinements in gamma transition theories and test of nuclear models [1-5]. However, there is not enough information on the formation of isomeric states and some discrepancies are observed among the literature values which might be attributed to variations in experimental methods and/or the nuclear constants used.

Since many years, the isomeric yield ratios have been subjected to extensive studies for better understanding of the mechanism of such reactions leading to the residual nuclei with an isomeric state and unstable ground state. Most of the experiments have been done for the nuclear reactions induced by incident particles, especially with neutrons around 14 MeV [5-8]. The measurements with bremsstrahlung photons are rare and were carried out mainly for simple reactions at low energies [9]. This is due to the lack of intense photon sources and the inherent background problems at photon beams [10]. Although the bremsstrahlung photons carry relatively small momentum, it is a good tool for

† Corresponding author. Tel.: +82 53 950 5320; fax: +82 53 939-3972. E-mail address: gnkim@knu.ac.kr (G. N. Kim)

investigating the dependences of isomeric yield ratios as a function of the incident photon energy and the mass difference (ΔA) between the product (A_p) and the target nucleus (A_t) [11].

In this work we have chosen the $^{nat}Fe(\gamma,xn1p)^{52m,g}Mn$ reaction for study. Iron and iron alloy are the most common materials in everyday life. Iron has important role in broad range of applications such as constructional material in different branches of industry, and in accelerator and reactor construction. In addition, the isomeric yield ratio for the $^{nat}Fe(\gamma,xnyp)^{52m,g}Mn$ reaction are very scanty. Kato and Oka [12] measured the isomeric yield ratio for the $^{nat}Fe(\gamma,xn1p)^{52m,g}Mn$ reaction by means of bremsstrahlung irradiation with maximum energies ranging from 30 to 72 MeV. Henry and Martin, Jr measured relative yields of $^{54}Fe(\gamma,2n)^{52}Fe$: $^{54}Fe(\gamma,pn)^{52}Mn$: $^{54}Fe(\gamma,pn)^{52m}Mn$ by irradiating with 70-MeV bremsstrahlung [13]. Walters and Hummel [14] also measured the isomeric yield ratio for the production of the ^{52}Mn isomer from iron by irradiated with bremsstrahlung of maximum energy in the 100- to 300-MeV range. di Napoli et al., [15] also gave one average data measured in the energy region 300-1000 MeV. In the GeV energy region we have found only one data for the $^{nat}Fe(\gamma,xn1p)^{52m,g}Mn$ reaction measured by activation method at 1.5 GeV bremsstrahlung energy by Kumbartzki and Kim [16]. Recently, we also measured the isomeric yield ratio for the $^{nat}Fe(\gamma,xn1p)^{52m,g}Mn$ reaction with 65-MeV bremsstrahlung [17].

The aim of the present work is to extend our measurements to higher incident photon energy up to 2.5-GeV, and to understand the dependency of the incident bremsstrahlung energy and the mass difference (ΔA) between the product (A_p) and the target nucleus (A_t) [11]. The experiment was done at the electron linac of Pohang Neutron Facility (PNF) [18, 19] and 2.5-GeV electron linac of the Pohang Accelerator Laboratory (PAL) [20, 21].

2. Experimental procedure

2.1. Bremsstrahlung radiation sources

The 50-, 60-, and 70-MeV bremsstrahlung beams were produced from the electron linac of PNF. The electron linac was designed for 100-MeV and can be operated from 40- to 70-MeV. The details of the electron linac and bremsstrahlung production are described elsewhere [18, 19]. The bremsstrahlung was produced when a pulsed electron beam hit a thin W target with a size of 100 mm × 100 mm and a thickness of 0.1 mm. The W target is located at 18 cm from the beam exit window.

The experiment with 2.5-GeV bremsstrahlung was carried out at the 10^o beam line of the main electron linac of the PAL [22]. The details of the 2.5-GeV electron linac and its applications were described elsewhere [20, 21]. The 2.5-GeV bremsstrahlung photons were produced when a pulsed electron beam hit a thin W target with a size of 50 mm × 50 mm and a thickness of 0.2 mm. The W target is located at 38.5 cm from the beam exit window.

2.2. Sample irradiation

A high-purity (99.559%) iron foil with a natural isotopic composition (^{54}Fe-5.8%, ^{56}Fe-91.72%, ^{57}Fe-2.2%, ^{58}Fe-0.28%) made by Reactor Experiments Inc. (USA) was used for the irradiation. The diameter of all foils was 12.7 mm and thickness was 0.127 mm. The iron foils were placed in air and positioned perpendicular to the direction of the electron beam. The iron foils were irradiated by the four different bremsstrahlung energies as follows: 4-h, 3-h, 3-h, and 4-h irradiations for 50-, 60-, 70-MeV, and 2.5-GeV bremsstrahlung energies, respectively. During the irradiation, the electron linac of the PNF was operated with a repetition rate of 15 Hz and a pulse width of 2 μs, and the 2.5-GeV electron linac was operated with a repetition rate of 10 Hz and a pulse width of 1 ns.

2.3. Activity measurements

After an irradiation and an appropriate waiting time, the foils were taken off, and then the induced gamma activities of the irradiated foils were measured by using a γ-spectrometer, without any chemical purification. The γ-spectrometer used for the measurements was a coaxial CANBERRA high-purity germanium (HPGe) detector with a diameter of 60.5 mm and length of 31 mm. The HPGe detector was coupled to a computer-based multichannel analyzer card system, which could determine the photopeak-area of the γ-ray spectra by using the GENIE2000 (Canberra) computer program. The energy resolution of the detector was 1.80 keV full width at half maximum (FWHM) at the 1332.5 keV peak of ^{60}Co. The detection efficiency was 20% at 1332.5 keV relative to a 3" diameter × 3" length NaI(Tl) detector. The photopeak efficiency curve of the gamma spectrometer was calibrated with a set of standard gamma sources: ^{241}Am (59.541 keV), ^{137}Cs (661.657 keV), ^{54}Mn (834.848 keV), ^{60}Co (1173.237 keV and 1332.501 keV), and ^{133}Ba (80.997 keV, 276.398 keV, 302.853 keV, 356.017 and 383.815 keV). The measured detection efficiencies were fitted by using the following function:

$$\ln \varepsilon = \sum_{n=0}^{5} a_n \left(\ln\left(E / E_0\right)\right)^n \tag{1}$$

where ε is the detection efficiency, a_n represents the fitting parameters, and E is the energy of the photopeak, and E_0 = 1 keV. The detection efficiencies as a function of the photon energy measured at different distances between the gamma source and the surface of the detector were illustrated in [17, 23].

The waiting and the measuring times were chosen based on the activity and the half-life of each radioactive isotope. In order to optimize the dead time and the coincidence summing effect we have also chosen the appropriate distance between the sample and the detector for each measurement. The activated foil was attached on a plastic sample holder and can be set at a distance from 5 mm to 105 mm from the surface of the HPGe detector. Generally, the dead times were kept below 2% during the measurement and the statistical errors below 5%. Measured typical γ-ray spectra of the iron foil irradiated with 70-MeV and 2.5-GeV bremsstrahlung are given in Fig. 1.

To measure the activities of the reaction products formed via the ^{nat}Fe(γ,xn1p)^{52m,g}Mn reaction we have chosen the γ-rays with high intensity and well separated. The activity of the irradiated foils is determined from the peak area of γ-ray and the detection efficiency at the peak energy. If the pulse nature of the irradiation sources is considered, the relation between the number of detected γ-rays, N_{obs}, and the reaction cross-section σ can be expressed as follows:

$$N_{obs} = \frac{N_0 \phi \sigma \varepsilon I_\gamma (1 - e^{-\lambda\tau})(1 - e^{-\lambda t_i}) e^{-\lambda t_w} (1 - e^{-\lambda t_c})}{\lambda (1 - e^{-\lambda T})} , \tag{2}$$

where N_0 is the number of target nuclei, ϕ is the incident photon flux, ε is the detection efficiency for the measured γ-ray, I_γ is the branching ratio or intensity of the γ-ray, λ is the decay constant of the isotope of interest ($\lambda = ln2/T_{1/2}$), τ is the pulse width, t_i is the irradiation time, t_w is the waiting time (the period between the end of irradiation and the start of counting), t_c is the measuring time, and T is the cycle period.

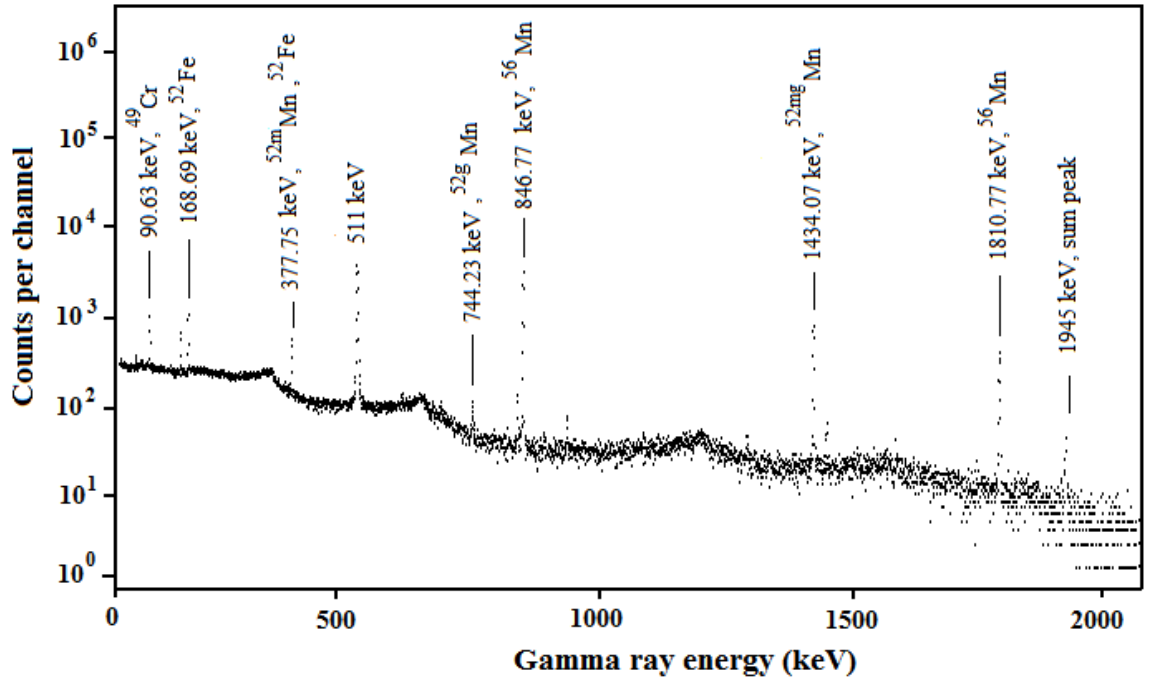

(a)

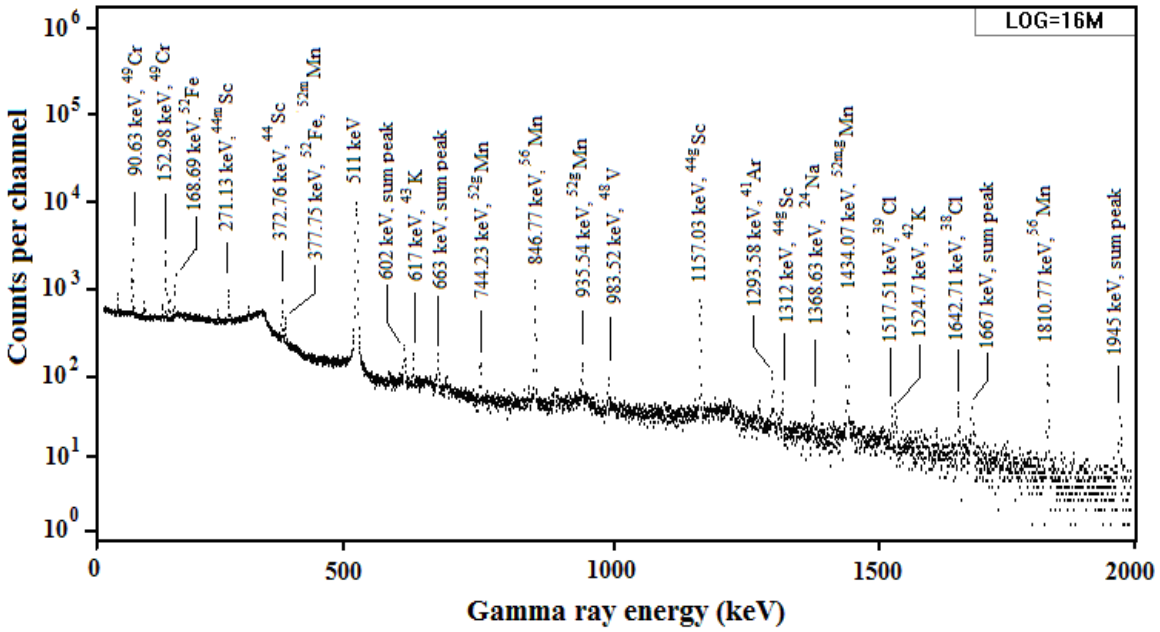

(b)

Fig. 1. Typical γ-ray spectra from the natural Fe foil irradiated with (a) 70 MeV (t_i = 3 h, t_w = 44 min, t_c = 30 min) and (b) 2.5 GeV (t_i = 4 h , t_w = 40 min, t_c = 10 min) bremsstrahlung.

3. Data analysis

3.1. Basic equations for isomeric yield ratio

The cross-section for the formation of an isomeric-state relative to that of ground-state is called the isomeric cross-section ratio. In case of the bremsstrahlung photon irradiation, due to the continuity of the energy spectrum, the isomeric cross-section ratio can also be represented through the

yields of the two states instead of two cross-sections. The yield of the isomeric- and the ground-state can be expressed as follows:

$$Y_i = N_0 \int_{E_{th}}^{E_{\gamma\max}} \sigma_i(E)\phi(E)dE \ , \tag{3}$$

where i represents the isomeric-state (m) or the ground-state (g) of a isomeric pair product of interest, N_0 is the number of target nuclei, $\sigma_i(E)$ is the energy dependent reaction cross-section and $\phi(E)$ is the shape of the bremsstrahlung spectrum. $E_{\gamma\max}$ and E_{th} are the maximum end point energy of bremsstrahlung and the reaction threshold, respectively.

By taking into account the fact that the ground-state radionuclide may be formed in two ways, directly from the target nuclide and/or indirectly through the decay of the isomeric nuclide, the production of a given isomeric pair and its decay during the activation time, t_i, can be described by the following differential equations:

$$\frac{dN_m}{dt} = Y_m - \lambda_m N_m \,, \tag{4}$$

$$\frac{dN_g}{dt} = Y_g - \lambda_g N_g + P\,\lambda_m N_m \,, \tag{5}$$

where N_i is the numbers of nuclei for i (= m, g) state, λ_m and λ_g are the decay constants of these states, and P is the branching ratio for the decay of the isomeric-state to the ground-state.

By solving equations (4) and (5) in the three time intervals (the activation time t_i, the waiting time t_w, and the counting time t_c) with consideration of the fact that the samples were irradiated by the pulsed bremsstrahlung beam, we can derive the isomeric ratio IR from the measured gamma activities as follows:

$$IR \equiv \frac{\sigma_m}{\sigma_g} = \left[\left(\frac{S_g}{S_m} \times \frac{\varepsilon_m I_{\gamma m}}{\varepsilon_g I_{\gamma g}} - \frac{P\lambda_g}{\lambda_g - \lambda_m} \right) \times \frac{A_m B_m C_m D_m}{A_g B_g C_g D_g} + \frac{P\lambda_m}{\lambda_g - \lambda_m} \right]^{-1} , \tag{6}$$

where S_m and S_g are the photopeak areas for the detected γ-rays of the isomeric-state and the ground-state, ε_i is the detection efficiency for the γ-ray of interest, I_γ is the γ-ray intensity, λ_i is the decay constant of the i state ($\lambda = \ln 2/T_{1/2}$ where $T_{1/2}$ is the half-life of the radioactive isotope), and the other parameters are

$$A_m = \frac{1-e^{-\lambda_m \tau}}{1-e^{-\lambda_m T}} e^{-\lambda_m (T-\tau)},\ B_m = \frac{1-e^{-\lambda_m t_i}}{\lambda_m},\ C_m = e^{-\lambda_m t_w},\ D_m = 1-e^{-\lambda_m t_c},$$

$$A_g = \frac{1-e^{-\lambda_g \tau}}{1-e^{-\lambda_g T}} e^{-\lambda_g (T-\tau)},\ B_g = \frac{1-e^{-\lambda_g t_i}}{\lambda_g},\ C_g = e^{-\lambda_g t_w},\ D_g = 1-e^{-\lambda_g t_c},$$

with τ being the pulse width or the real irradiation time in the cycle period, t_i the irradiation time, which is the time difference between the start and the stop of irradiation, t_w the waiting time or the time between the end of irradiation and the start of counting, t_c the counting or measuring time, and T

the cycle period. As we can see from Eq. (6), it is not necessary to measure the photon flux density because the isomeric pair was formed at the same reaction threshold.

3.2. Determination of isomeric yield ratio

The ^{52m,g}Mn isomeric pairs were identified based on their characteristic γ-ray energies and half-lives. The nuclear reactions and decay data of the ^{52m,g}Mn are taken from [24] and given in Table 1. The simplified level and decay scheme of the ^{52m,g}Mn is given in Fig. 2. The isomeric-state ^{52m}Mn (low-spin state, 2^+) with a half-life of 21.1 min decays directly to the 1434.09 keV state of ^{52}Cr (2^+) by both β^+ and electron-capture (EC) processes with a branching ratio of 98.0%. Meanwhile, only 1.75% of the isomeric-state decays to the unstable ground-state ^{52g}Mn (high-spin state, 6^+) by emitting the 377.74 keV γ-ray. The unstable ground-state ^{52g}Mn (6^+) with a half-life of 5.591d decays to the 3615.92 keV state of ^{52}Cr (5^+) by EC process with a branching ratio of 7.69%, and also to the 3113.86 keV state of ^{52}Cr (6^+) by both a β^+ and an EC process with a branching ratio of 91.4%. By considering the γ-ray intensity and energy as well as the possible interferences, the activity of the isomeric-state ^{52m}Mn was determined based on the 1434.3 keV γ-peak. We did not use the 377.74 keV γ-ray for ^{52m}Mn since its intensity is rather low (1.68%). In addition, the 377.74 keV γ-ray of ^{52m}Mn is also disturbed by the 377.75 keV (1.64%) γ-ray of ^{52}Fe isotope formed via the ^{nat}Fe(γ,xn)^{52}Fe reactions and by the 377.88 keV (42%) γ-ray of ^{53}Fe isotope formed via the ^{nat}Fe(γ,x'n)^{53}Fe reactions. The activity of the unstable ground-state ^{52g}Mn was determined by using the γ-ray of 744.23 keV.

Table 1: Nuclear reactions investigated and decay data of reaction product, ^{52m,g}Mn [24].

Nuclear Reaction	Threshold energy E_{th} [MeV]	Half-life $T_{1/2}$	γ-ray energy E_γ [keV]	γ-ray intensity I_γ [%]
^{nat}Fe(γ,xn1p) ^{52m}Mn	40.70	21.1 min	377.75	1.68
			1434.07*	98.29
			1727.53	0.22
^{nat}Fe(γ,xn1p)^{52g}Mn	40.32	5.591 d	744.23*	90.64
			935.54	94.9
			1333.64	5.07
			1434.07	100

* γ-rays used in calculations

As we can see from the γ-ray spectra in Figs. 1 (a) and 1 (b) and decay scheme in Fig. 2, the 744.23 keV photopeak is well separated, but the 1434.07 keV photopeak is a mixture of the ^{52m}Mn and the ^{52g}Mn radionuclide. In order to determine the activity of the ^{52m}Mn isotope by using the 1434.07 keV photopeak, we have to subtract the contribution from the ^{52g}Mn. In the present work, the activity contribution from the ^{52g}Mn to the ^{52m}Mn was derived by measuring and analysing the decay curve of the 1434.07 keV photopeak. The analysis method was done by the same way as described in our previous work [25].

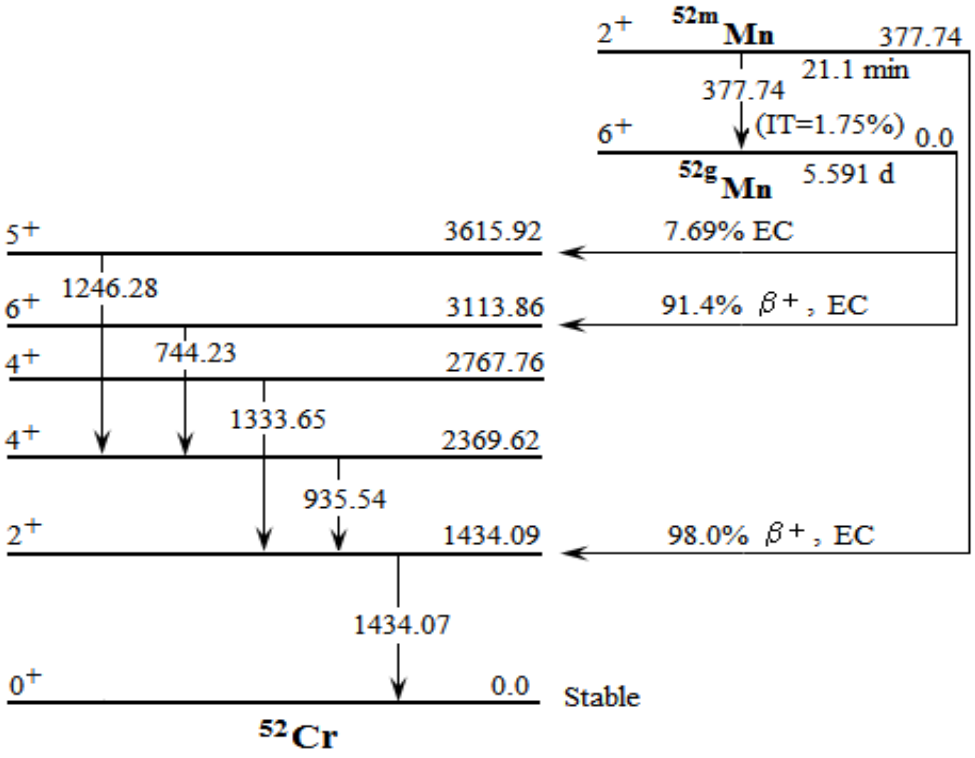

Fig. 2. Simplified decay scheme of the isomeric pair ^{52m,g}Mn. The nuclear level energies are in keV.

The main photonuclear reactions leading to the ^{52m,g}Mn isomeric pairs are as follows: ^{54}Fe(γ,np)^{52m,g}Mn, ^{56}Fe(γ,p3n)^{52m,g}Mn, and ^{57}Fe(γ,p4n)^{52m,g}Mn. In addition, the ^{52m}Mn can also be produced from the decay of ^{52}Fe ($T_{1/2}$ = 8.275 h) formed via the ^{54}Fe(γ,2n), ^{56}Fe(γ,4n), ^{57}Fe(γ,5n), and ^{58}Fe(γ,6n) reactions with threshold energies of 24.07-, 44.58-, 52.23-, and 62.28-MeV, respectively. A ^{52}Fe decays to a ^{52m}Mn by positron emission and by electron capture with a branching ratio of 55.49% and 44.57%, respectively. This is followed by a γ-ray of 168.69 keV (99.2%) leading to ^{52m}Mn. ^{52m}Mn decays in two branches, with 98% goes to stable ^{52}Cr and 1.75% goes to ^{52g}Mn. Therefore, the contribution from the ^{52}Fe was corrected when we measured the activity of ^{52m,g}Mn.

The isomeric pair ^{52m,g}Mn emits multiple γ-rays, and some of them are in cascade with the γ-rays used in calculations, namely the 744.23 keV and 1434.07 keV. In order to obtain accurate results the true coincidence summing (also called cascade summing) factor was determined, and it was used for correcting the measured activity. The 744.23 keV γ-ray from the ^{52g}Mn is in coincidence with the 935.54 keV and the 1434.07 keV γ-rays (triple cascade). The 1434.07 keV γ-ray from the ^{52m}Mn is in coincidence with the 511 keV annihilation photons (from β^+ decay of the ^{52m}Mn). The true coincidence summing factors were calculated based on the measured total and absolute photopeak efficiencies and the formulae for complex decay schemes [26-28]. By neglecting the triple cascade summing effect, the true coincidence summing factors calculated at 2.5 cm distance from the sample to the HPGe detector were 1.107 and 1.081 for the 744.23 keV and 1434.07 keV γ-rays, respectively.

After activity measurements and making necessary corrections, we calculated the isomeric yield ratio by using the equation (6).

4. Results and discussion

The isomeric yield ratios for the ^{52m,g}Mn isomeric pair formed by the ^{nat}Fe(γ,xn1p)^{52m,g}Mn reaction induced by 50-, 60-, 70-MeV, and 2.5-GeV bremsstrahlung were determined from the measured activities of the high-spin state (^{52g}Mn: 6^+) to that of the low-spin state (^{52m}Mn: 2^+). The obtained isomeric yield ratios for the ^{nat}Fe(γ,xn1p)^{52m,g}Mn reaction measured at 50-, 60-, 70-MeV and 2.5-GeV bremsstrahlung, together with the available data from other authors [12-17], are summarized in Table 2.

Table 2: Isomeric yield ratios for the ^{nat}Fe(γ,xn1p)^{52m,g}Mn reaction induced by different photon energy.

Nuclear reaction	Photon energy [MeV]	Isomeric yield ratio, $R=Y_{high\text{-}spin}/Y_{low\text{-}spin}$	
		Present work	Existing Results
^{nat}Fe(γ,xn1p)^{52m,g}Mn	30	-	0.102 [12]
	50	0.27±0.03	-
	60	0.33±0.04	-
	65	-	0.28±0.04 [17]
	70	0.34±0.04	0.32±0.05 [13]
	100	-	0.39±0.03 [14]
	150	-	0.36±0.02 [14]
	200	-	0.35±0.02 [14]
	250	-	0.37±0.02 [14]
	300-1000	-	1.3 ± 0.8 [15]
	1500	-	0.87±0.1 [16]
	2500	1.25±0.15	-

The present results at 50- and 60-MeV as well as 2.5-GeV bremsstrahlung energies are the first measurements. The main sources of the errors are due to uncertainties in photopeak efficiency calibration (~4%), intensities of the γ-rays (0.4-2%), photopeak area determination (2-4.2%), and coincidence summing effect (3-3.5%). The total uncertainties in the present results have been obtained by combining the sub-total uncertainties for the isomeric state (m) and the ground state (g) listed in Table 3.

The present isomeric yield ratios for the ^{nat}Fe(γ,xn1p)^{52m,g}Mn reaction together with the available data from other experiments are plotted as a function of the energy of the incident bremsstrahlung, as shown in Fig. 3. The isomeric yield ratio of Kato and Oka [12] measured at 30-MeV is lower than the present results measured in the energy region 50-70 MeV. The value measured by Kato and Oka [12] probably represents only for the ^{52m,g}Mn isomeric pair formed through the ^{54}Fe(γ,np) reaction because of the 30-MeV bremsstrahlung energy. In general, the ^{52m,g}Mn can be formed from ^{54}Fe(γ,np), ^{56}Fe(γ,3np), ^{57}Fe(γ,4np) and ^{58}Fe(γ,5np) with threshold energies of about 21-MeV, 41-MeV, 49-MeV and 59-MeV, respectively. Walters et al. [29] measured the isomeric yield ratio for the ^{54}Fe(γ,np) ^{52m,g}Mn reaction only at 250 MeV bremsstrahlung energy and showed that only 17% of ^{52m,g}Mn is produced by the ^{54}Fe(γ,np) reaction in a natural iron target. The present result measured at 70-MeV bremsstrahlung is consistent with that measured by Henry et al. [13] within the error. However, there are no data in literature for direct comparison with our results at 50-, 60-MeV, and 2.5-GeV bremsstrahlung energies.

Table 3: Uncertainty sources and their values in the isomeric yield ratio measurements for the ^{52m,g}Mn isomeric pairs at 50-, 60-, 70-MeV and 2.5-GeV bremsstrahlung energy.

Source of uncertainty	Uncertainties (%)							
	50-MeV		60-MeV		70-MeV		2.5-GeV	
	m	g	m	g	m	g	m	g
Statistical error	2.0	2.0	2.0	2.0	2.0	2.0	2.0	2.0
Detection efficiency	4.0	4.0	4.0	4.0	4.0	4.0	4.0	4.0
Half-life	1.0	0.05	1.0	0.05	1.0	0.05	1.0	0.05
Gamma intensity (%)	2.0	0.4	2.0	0.4	2.0	0.4	2.0	0.4
Coincidence summing effect	3.5	3.0	3.5	3.0	3.5	3.0	3.5	3.0
Net peak area fitting	4.0	2.0	4.0	2.5	4.0	2.0	4.2	3.0
Gamma ray self-absorption	0.5	1.0	0.5	1.0	0.5	1.0	0.5	1.0
Others	4.5	4.0	5.5	5.0	5.5	5.0	5.5	5.0
Sub-total uncertainty	8.6	7.1	9.2	7.8	9.2	7.7	9.2	8.0
Total uncertainty	***11.2***		***12.1***		***12.0***		***12.2***	

As can be seen in Fig. 3, the isomeric yield ratios increase with the increasing bremsstrahlung energies from the threshold up to about 100 MeV. In the energy region from 100-MeV to 250-MeV the isomeric yield ratios seem to be saturated. Unfortunately, there are no data in literature in the region from 250-MeV to 1-GeV bremsstrahlung energy. At higher bremsstrahlung energy region, 1-2.5 GeV, we can see that the isomeric yield ratio for the ^{nat}Fe(γ,np)^{52m,g}Mn reaction is slightly increase with the increasing bremsstrahlung energies.

There are several isomeric yield ratios for the ^{52m,g}Mn isomeric pairs formed by different reaction channels at GeV-regions, such as ^{55}Mn(γ,3n)^{52m,g}Mn [30], ^{nat}Fe(γ,xnp)^{52m,g}Mn [15,16], ^{59}Co(γ,5n2p)^{52m,g}Mn [15,33] and ^{nat}Cu(γ,xn4p)^{52m,g}Mn [31,34]. The isomeric yield ratios for the ^{52m,g}Mn isomeric pairs formed by different reaction channels at GeV-regions are plotted as a function of the mass difference (ΔA) between the product and the target nucleus, as shown in Fig. 4. We can see that the isomeric yield ratio increases gradually with the increasing mass difference or with the number of nucleons emitted. It is seems that the isomeric yield ratios for the ^{52m,g}Mn isomeric pairs formed in different reaction channels in the GeV bremsstrahlung energy region increase gradually with the complexity of the (γ,xnyp) photonuclear reactions. The relation between the isomeric yield ratio and the mass difference (ΔA) for the ^{52m,g}Mn isomeric pairs formed in different reaction channels with bremsstrahlung in the energy range 1-4 GeV can be approximated by the same expression given in our previous report [22] for the ^{44m,g}Sc isomeric pairs as follows: $IR = k \times (1 - \exp(-\alpha \times \Delta A))$, where k =0.012 and α=27.35.

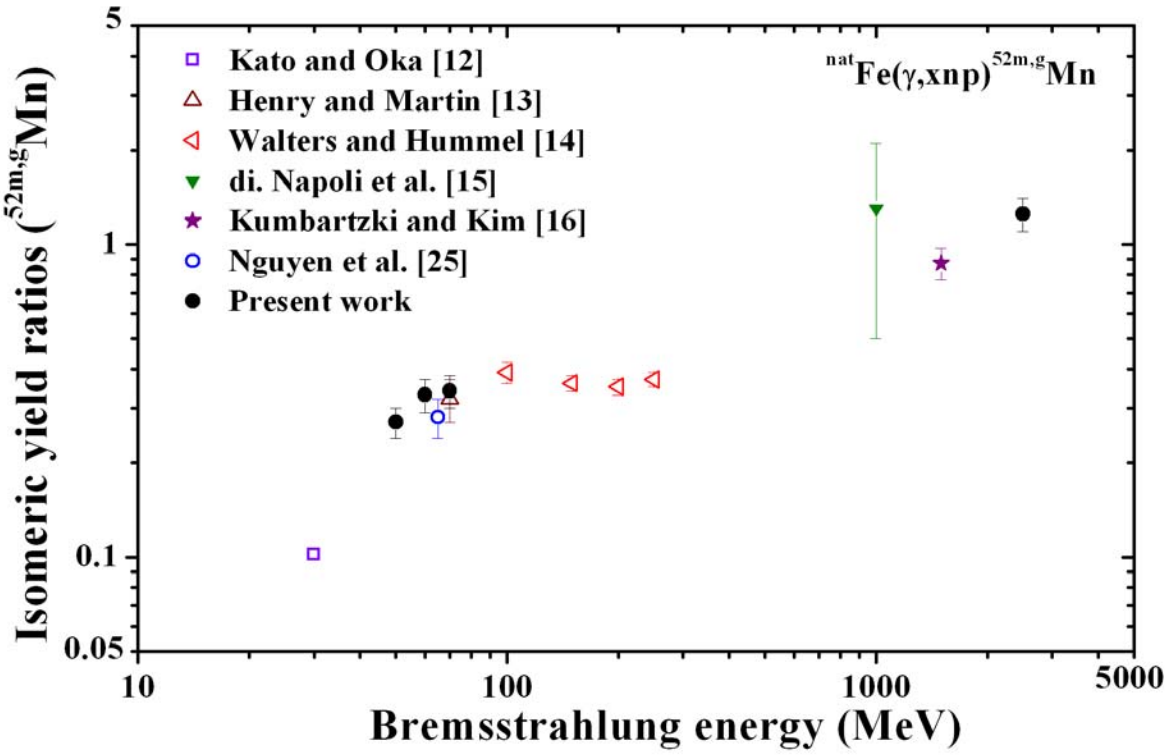

Fig. 3: Dependence of the isomeric yield ratios on the incident bremsstrahlung energies for the $^{nat}Fe(\gamma,xnp)^{52m,g}Fe$ reaction.

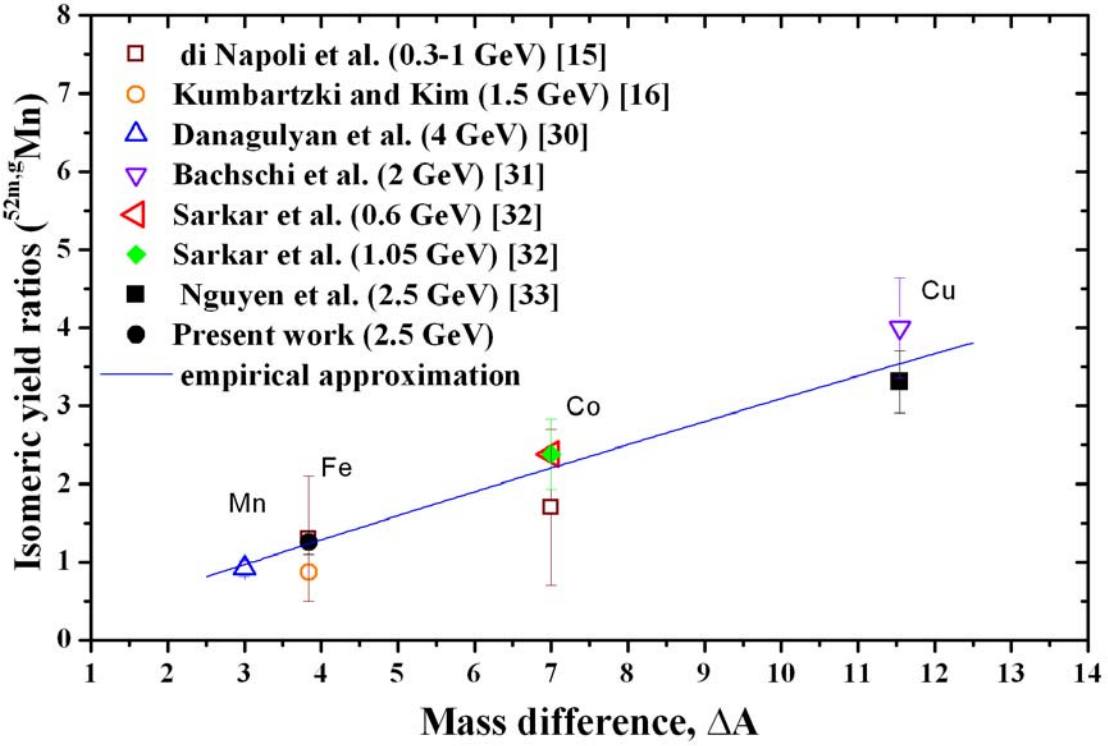

Fig. 4: Isomeric yield ratios of $^{52m,g}Mn$ formed in different targets: Mn, Fe, Co and Cu with bremsstrahlung in the energy range 1-5 GeV as a function of mass difference, ΔA.

5. Conclusion

We have measured the isomeric yield ratios for the $^{nat}Fe(\gamma,xnyp)^{52m,g}Mn$ reaction at 50-, 60-, 70-MeV and 2.5-GeV bremsstrahlung energies. The present results at 50-, 60-MeV and 2.5-GeV are the first measurements. The present result measured at 70-MeV bremstrahlung is consistent with the value measured by Henry and Martin, Jr [13]. From the present results and the data existing in literature we observed that the isomeric yield ratio for the $^{52m,g}Mn$ isomeric pairs formed in multi-particle photonuclear reactions depends on the incident bremsstrahlung energy, especially in the GeV-energy region.

The isomeric yield ratios for the $^{52m,g}Mn$ isomeric pairs formed by different reaction channels $^{55}Mn(\gamma,3n)^{52m,g}Mn$, $^{nat}Fe(\gamma,np)^{52m,g}Mn$, $^{59}Co(\gamma,5n2p)^{52m,g}Mn$, and $^{nat}Cu(\gamma,xn4p)^{52m,g}Mn$ at GeV-energy region increase with an increase of the mass difference (ΔA). This can be explained as the momentum transfer, which is more probable for complex photonuclear reactions.

Acknowledgements

The authors would like to express their sincere thanks to the staffs of Pohang Accelerator Laboratory for excellent operation of the electron linac and their strong support. This work was supported by the Korea Science and Engineering Foundation (KOSEF) through a grant provided by the Korean Ministry of Education, Science and Technology (MEST) in 2008 (Project No. M2 08B090010810), by the Institutional Activity Program of Korea Atomic Research Institute, and by the Vietnam National Foundation for Science and Technology Development (NAFOSTED).

References

[1] J.R. Huizenga, R. Vandenbosch, Phys. Rev. **120** (1960) 1305; R. Vandenbosch, R. Huizenga, Phys. Rev. **120** (1960) 1313.
[2] H.A. Bethe, Rev. Mod. Phys. **9** (1937) 84.
[3] C. Bloch, Phys. Rev. **93** (1954) 1094.
[4] K.J. Le Couteur, D.W. Lang, Nucl. Phys. **13** (1959) 32.
[5] R. Vanska, R. Rieppo, Nucl. Instr. and Meth. **179** (1981) 525.
[6] I.G. Birn, B. Strohmaier, H. Freiesleben, S.M. Qaim, Phys. Rev. **C 52** (1995) 2546; S.M. Qaim, Nucl. Phys. **A185** (1972) 614; S.M. Qaim, Nucl. Phys. **A 438** (1985) 384; C.D. Nesaraja, S. Sudar, S.M. Qaim, Phys. Rev. **C 68** (2003) 024603.
[7] R. Sarkar, V.N. Bhoraskar, Phys. Rev. **C 46** (1992) 2246.
[8] I. A. Reyhancan, M. Bostan, A. Durusoy, A. Elmali, A. Baykal, Y. Ozbir, Ann. Nucl. Energy **30** (2003) 1539.
[9] M. Eriksson, G.G. Jonsson, Nucl. Phys. **A 242** (1975) 507.
[10] W. Gunther, K. Huber, U. Kneissl, H. Krieger, Nucl. Phys. **A 297** (1978) 254.
[11] K. Lindgren, G.G. Jonsson, Nucl. Phys. A 166 (1971) 643.
[12] T. Kato, Y. Oka, Talanta **19** (1972) 515.
[13] R.M. Henry, D.S. Martin, Jr., Phys. Rev. **107** (1957) 772.
[14] W.B. Walters, J.P. Hummel, Phys. Rev. **150** (1966) 867.
[15] V. di Napoli, F. Salvetti, M.L. Terranova, H.G. De Carvalho, J.B. Martines, O.A.P. Tavares, J. Inorg. Nucl. Chem. **40** (1978) 175.
[16] G. Kumbartzki, U. Kim, Nucl. Phys. **A176** (1971) 23.
[17] V.D. Nguyen, D.K. Pham, T.T. Kim, D.T. Tran, V.D. Phung, Y.S. Lee, G.N. Kim, Y. Oh, H.S. Lee, H. Kang, M.H. Cho, I.S. Ko, W. Namkung, J. Korean Phys. Soc. 50 (2007) 417.

[18] G.N. Kim, Y.S. Lee, V. Skoy, V. Kovalchuck, M. H. Cho, I.S. Ko, and W. Namkung, D. W. Lee, H.D. Kim, T.I. Ro, and Y.G. Min, J. Korean Phys. Soc. **38** (2001) 14; G. N. Kim, H. Ahmed, R. Machrafi, D. Son, V. Skoy, Y.S. Lee, H. Kang, M. H. Cho, I.S. Ko, and W. Namkung, J. Korean Phys. Soc. **42** (2003) 479.
[19] V. D. Nguyen, D. K. Pham, D. T. Tran, V. D. Phung, Y.S. Lee, H.S. Lee, M.H. Cho, I.S. Ko, W. Namkung, A.K.M.M.H. Meaze, K. Devan, G.N. Kim, J. Korean Phys. Soc. **48** (2006) 382.
[20] H. S. Lee, S. Ban, T. Sato, K. Shin, J. S. Bak, C. W. Chung, H. D. Choi, J. Nucl. Sci. and Tech. S1 (2000) 207.
[21] T. Sato, K. Shin, R. Yuasa, S. Ban, H. S. Lee, Nucl. Instr. and Meth. A 463 (2001) 299.
[22] V.D. Nguyen, D. K. Pham, T. T. Kim, T. S. Le, Md. S. Rahman, K.S. Kim, M. Lee, G.N. Kim, Y. Oh, H.S. Lee, M.H. Cho, I.S. Ko, W. Namkung, Nucl. Instr. and Meth. **B 266** (2008) 5080.
[23] V.D. Nguyen, D. K. Pham, T. T. Kim, T. S. Le, Y.S. Lee, G.N. Kim, Y. Oh, H.S. Lee, M.H. Cho, I.S. Ko, W. Namkung, Nucl. Instr. and Meth. **B 266** (2008) 21.
[24] R.B. Firestone, C.M. Baglin, S.Y.F. Chu, Table of Isotopes, 8th edition. Update on CD Rom, Wiley-Interscience, New York, (1999).
[25] V. D. Nguyen, D. K. Pham, T. T. Kim, D. T. Tran, V. D. Phung, Y.S. Lee, G.N. Kim, Y. Oh, H.S. Lee, H. Kang, M.H. Cho, I.S. Ko, W. Namkung, J. Korean Phys. Soc., **50** (2007) 417.
[26] K. Debertin, R. G. Heimer, Gamma and X-ray spectrometry with semiconductor detectors, North Holland Elsevier, New York, 1988.
[27] M. de Bruin, P. J. M. Korthoven, Radiochem. Radioanal. Lett. **19** (1974) 153.
[28] V. D. Nguyen, D. K. Pham, T. T. Kim, T. S. Le, G. N. Kim, Y. S. Lee, Y. Oh, H. S. Lee, M. H. Cho, I. S. Ko, and W. Namkung, Nucl. Instr. and Meth. B 266 (2008) 863.
[29] W.B. Walters, J.R. Van Hise, W.L. Switzer, J.P. Hummel, Nucl. Phys. **A 157** (1970) 73.
[30] A.S. Danagulyan, N. A. Demekhina, G.A. Vartapetyan, Nucl. Phys. A 285 (1977) 482.
[31] N.M. Bachschi, P. David, J. Debrus, F. Lubke, H. Mommsen, R. Schoenmackers, G.G. Jonsson, K. Lindgren, Nucl. Phys. **A 264** (1976) 493.
[32] S.R.Sarkar, M. Soto, Y. Kubota, M. Yoshida, T. Fukasawa, M. Matsumoto, K. Kawaguchi, K. Sakamoto, S. Shibata, M. Furukawa, I. Fujiwara, Radiochim. Acta **55** (1991)113.
[33] V. D. Nguyen et al., to be published (2009).